

## Magnetic anisotropy of grain boundaries in nanocrystalline Ni



## ARTICLE INFO

## Keywords:

Grain boundary magnetic anisotropy  
Uniaxial anisotropy  
Cubic anisotropy  
Nanocrystalline materials  
Landau–Lifshitz–Gilbert theory

## ABSTRACT

Temperature-dependent magnetic anisotropy due to grain boundaries in nanocrystalline Ni has been studied by simulating experimental magnetization data with the stochastic Landau–Lifshitz–Gilbert theory. In the model the grain boundary magnetic anisotropy energy is expressed as the sum of the uniaxial anisotropy and the cubic anisotropy, characterized by  $K_{ua}$  and  $K_{ca}$  anisotropy constants. By comparing the calculated magnetization with the experimental magnetization measurements at finite temperatures, the values of  $K_{ua}$  and  $K_{ca}$  can be determined. For nanocrystalline Ni it is found that with increasing temperature  $K_{ua}$  decreases and  $K_{ca}$  increases. At low temperatures  $K_{ua}$  dominates the grain boundary anisotropy energy, whereas  $K_{ca}$  is very small and it can be neglected. At room temperature  $K_{ua}$  and  $K_{ca}$  are of the same order with the corresponding ratio  $K_{ua}/K_{ca} \approx 1.9$ , both coefficients are much larger than the magnetocrystalline anisotropy constant.

© 2016 Elsevier B.V. All rights reserved.

## 1. Introduction

Surface effects play an important role in the magnetic properties of ferromagnetic particle systems and the influence of surface is dominant when the particle size decreases to the nanometer scale [1]. Experimental studies of assemblies of magnetic nanoparticles show that the magnetic anisotropy increases with decreasing particle size due to the contribution from surface anisotropy [2–6]. The surface anisotropy constant  $K_s$ , defined as the volume density of the surface anisotropy energy, can be determined from the phenomenological formula of Bodker and co-workers [2]:

$$K_{eff} = K_c + \frac{6}{D}K_s, \quad (1)$$

which requires the determination of the effective anisotropy constant  $K_{eff}$  by the measurements of thermally activated magnetic viscosity [7] or the dynamic measurements of magnetic susceptibility [8]. Here,  $D$  is the diameter of the particles and  $K_c$  is the core magnetocrystalline anisotropy. Validity of Eq. (1) has been questioned because it is based on the assumption that the contributions of the core and surface of nanoparticles to the total effective anisotropy are simply additive and the equation neglects the crosslinked effects [9,10]. It has also been demonstrated that Eq. (1) is restricted to the interacting systems where the interparticle interactions are significant [11].

Theoretical studies have shown that a cluster of atoms with many spins can be represented as a single-domain particle with an effective magnetic moment  $\vec{m}$  [5,9,12–14]. The surface-induced magnetic anisotropy energy  $E_s$  of the cluster can be expressed as:

$$E_s = -K_{ua}\hat{m}_z^2 + K_{ca}(\hat{m}_x^4 + \hat{m}_y^4 + \hat{m}_z^4), \quad (2)$$

where  $\hat{m}_\alpha$  ( $\alpha = x, y, z$ ) are the Cartesian components of the unit vector along the moment direction,  $K_{ua}$  and  $K_{ca}$  are the anisotropy constants representing the first-order surface anisotropy (FOS), arising from the broken symmetry of crystal environment and missing neighbours, and the second-order surface anisotropy (SOS), caused by the deviation of atomic spins on the surface from the collinearity of the core spins of the cluster due to the competition of the surface anisotropy and the exchange interactions. In practice it is difficult to determine FOS and SOS contributions to the surface anisotropy with sufficient precision [13]. Jamet and co-workers [15] and Kachkachi and Bonet [13] suggested using micro-SQUID technique to measure the switching field of a single cluster along various crystallographic directions and then fitting the experimental results with the pre-assumed anisotropy energy function with different values of FOS and SOS.

Similar to the effect of the surface in magnetic properties of nano-particle systems, grain boundaries in nanocrystalline (nc) materials induce the strong magnetic anisotropy due to the breaking of the symmetry of the atoms in these regions, termed here the grain boundary anisotropy. For magnetic nc materials, the SOS anisotropy arising from the non-collinearity of atomic spins at the grain boundaries with respect to the grain interiors, is large at finite temperatures [16]. For nc-Ni, it has been found that at low temperatures the grain boundary anisotropy energy can be represented by a uniaxial term, whereas the SOS anisotropy is very small and it can be neglected [19]. As temperature increases, the contribution from the thermal energy reduces the intensity of spin exchange interactions in the grains inducing the significant

deviation of the grain boundary spins from the moment direction of the atoms inside the grain. As a result one observes a substantial increase of SOS anisotropy energy at higher temperatures [16].

At the moment, we have no quantitative understanding of the contribution of grain boundary anisotropies to the magnetic properties of nc materials, since there is no suitable technique which permits measurement of these effects. The suggested micro-SQUID method [15,13] cannot be used to differentiate between SOS and FOS. Also, the magnetic interactions between individual grains are strong in nc materials, and the Stoner–Wohlfarth theory [17], applicable only to the non-interacting magnetic moments, cannot be used to obtain these properties from modelling studies. [19,16]. The method relies on the application of stochastic Landau–Lifshitz–Gilbert (LLG) model of magnetization dynamics [18] incorporating the anisotropy energy as per Eq. (2), and it requires matching the theoretical calculations of the magnetization against measured magnetization hysteresis data across different temperatures. [19,16].

## 2. Results and discussion

The experimental procedure and characterization of the properties of nc-Ni samples have been described in previous papers [19,16]. Nanocrystalline Ni foil of the thickness 50  $\mu\text{m}$  and grain size of 22.5 nm was produced by electrodeposition. The foil had a fiber texture with two dominant texture components, (200) and (111), aligned along the growth direction of the deposit, perpendicular to the surface of the foil. The volume fraction  $f_c$  of (200) and (111) texture components was 23% and 6% and the remaining fraction of the grains was oriented randomly in the plane of the foil. The samples for magnetic property measurements were punched from the nc-Ni foil and had diameter of 3 mm. The magnetic properties of nc-Ni samples were measured with a Quantum Design SQUID magnetometer in two directions of the applied field, parallel (in-plane) and perpendicular (out-of-plane) to the sample surface, at temperatures  $T=2$  K, 100 K and 298 K. Experimental magnetic hysteresis loops are shown in Figs. 1–3. At a given temperature, the difference in saturation magnetization  $M_s$  between the measurements in the two applied magnetic field directions is caused predominantly by the anisotropic dipolar interactions or the unsymmetrical sample shape.

The hysteresis loops at different temperatures have been

simulated using Landau–Lifshitz–Gilbert (LLG) theory of magnetization dynamics developed to model properties of nc materials. The method involves numerical solution of the stochastic LLG equation to determine the anisotropy constants as described by Eq. (2). Detailed procedure and setting of the numerical calculations are described in Refs. [16,19] and are briefly summarized in the following. The calculations for field-dependent magnetization are performed in Cartesian  $X, Y, Z$  space containing  $35 \times 35 \times 4$  uniform spherical grains with the diameter 22.5 nm equal to the average grain size and located on a simple cubic lattice with the lattice constant  $L_p = 22.2$  nm. A choice of  $L_p$ , being slightly smaller than the average grain size, is governed by the consideration of exchange interaction between neighboring grains [19]. The periodic boundary conditions along  $X$  and  $Y$  directions in the plane of the sample and fixed boundary in the  $Z$  direction perpendicular to the sample surface are applied to account for the geometry of the sample. The total energy  $E_{tot}$  of the modelling system includes the contributions from the external field  $\vec{H}_{ext}$ , magnetocrystalline and grain-boundary anisotropies, and dipolar and exchange interactions. At temperature  $T$  the total energy can be expressed as:

$$E_{tot} = -\mu_0 V M_s(T) \sum_{i=1}^N \hat{m}_i \cdot \vec{H}_{ext} + V \sum_{i=1}^N \left\{ K_c(T) \left( \hat{m}_{ix_i}^2 \hat{m}_{iy_i}^2 + \hat{m}_{ix_i}^2 \hat{m}_{iz_i}^2 + \hat{m}_{iy_i}^2 \hat{m}_{iz_i}^2 \right) + \left[ K_{ca}(T) \left( \hat{m}_{ix_i}^4 + \hat{m}_{iy_i}^4 + \hat{m}_{iz_i}^4 \right) - K_{ua}(T) \hat{m}_{iz_i}^2 \right] \right\} + \frac{\mu_0 M_s^2(T) V}{8\pi} h_d \sum_{i,j(i \neq j)}^N \left[ \frac{\hat{m}_i \cdot \hat{m}_j}{r_{ij}^3} - 3 \frac{(\hat{m}_i \cdot \hat{r}_{ij})(\hat{m}_j \cdot \hat{r}_{ij})}{r_{ij}^5} \right] - \frac{A_p(T)}{2L_p^2} V \sum_{\langle i,j \rangle} \hat{m}_i \cdot \hat{m}_j, \quad (3)$$

where  $\hat{m}_i$  and  $\vec{r}_i$  are the components of unit vector  $\hat{m}_i$  along the direction of magnetic moment  $\vec{m}_i$  of the  $i$ -th grain at the displacement  $\vec{r}_i$  in two local Cartesian coordinate systems respectively. Here,  $\hat{r}_{ij} = (\vec{r}_i - \vec{r}_j)/L_p$  with  $r_{ij} = |\hat{r}_{ij}|$  and  $N$  denotes the total number of grains in the sample.  $K_c(T)$  is the magnetocrystalline anisotropy constant whose values at different temperatures are taken from the experimental measurements of the bulk material [20,21].  $A_p(T)$  is the intergrain exchange constant introduced to characterize the

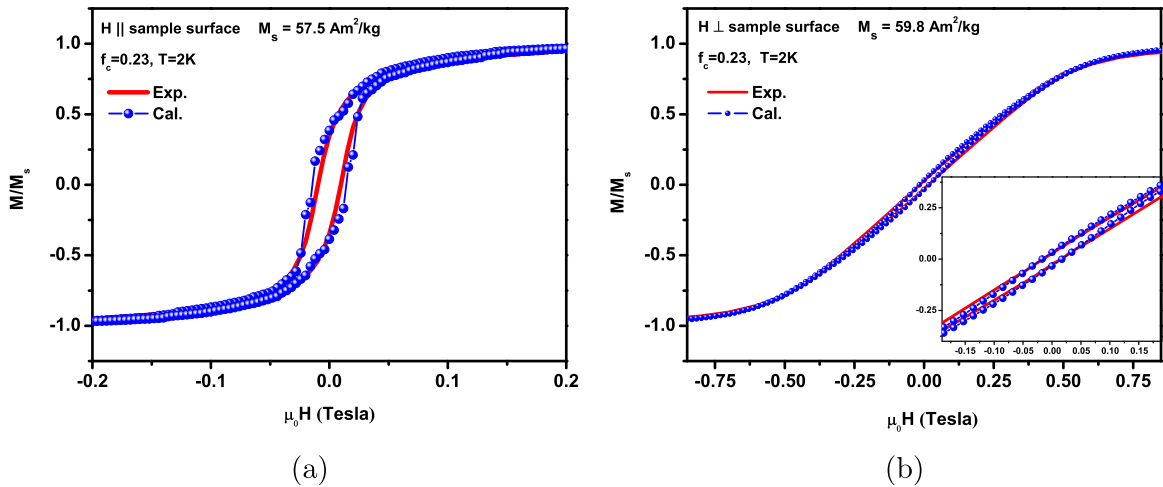


**Fig. 1.** Hysteresis loop of nc-Ni sample in the orientation of the magnetic field parallel (Fig. 1a) and perpendicular (Fig. 1b) to the sample surface at  $T=2$  K. The solid red curves are the experimental measurements with the saturation magnetization  $M_s = 57.5 \text{ Am}^2/\text{kg}$  and  $59.8 \text{ Am}^2/\text{kg}$  in the direction of the magnetic field parallel and perpendicular to the sample surface respectively. The point-dash blue curves represent the simulation results. (For interpretation of the references to color in this figure caption, the reader is referred to the web version of this paper.)

Download English Version:

<https://daneshyari.com/en/article/1797643>

Download Persian Version:

<https://daneshyari.com/article/1797643>

[Daneshyari.com](https://daneshyari.com)